Impact of the poly(propylene oxide)-*b*-poly(dimethylsiloxane)-*b*-poly-(propylene oxide) macrodiols on the surface-related properties of polyurethane copolymers

Ivan S. Stefanović[1], Dejan Gođevac[1], Milena Špírková[2], Petar Jovančić[3], Vele Tešević[4], Vesna Milačić[5], Marija V. Pergal[1]

[1]*Institute of Chemistry, Technology and Metallurgy (ICTM) – Center of Chemistry, University of Belgrade, Belgrade, Serbia*
[2]*Institute of Macromolecular Chemistry AS CR, v.v.i. (IMC), Prague , Czech Republic*
[3]*Faculty of Technology and Metallurgy, University of Belgrade, Belgrade, Serbia*
[4]*Faculty of Chemistry, University of Belgrade, Belgrade, Serbia*
[5]*North Campus Research Complex, B20, University of Michigan, Ann Arbor, MI 48109, USA*

Abstract

Segmented thermoplastic polyurethane copolymers (PURs) were synthesized using 4,4'--methylenediphenyl diisocyanate and 1,4-butanediol as the hard segment and *α*,*ω*-dihydroxy-poly(propylene oxide)-*b*-poly(dimethylsiloxane)-*b*-poly(propylene oxide) (PPO-PDMS) as the soft segment. The content of incorporated soft segments in PURs varied in the range from 40 to 90 wt.%. The structure, molecular weights and crystallinity of obtained copolymers were monitored by FTIR, ^{1}H- and 2D-NMR spectroscopy, and GPC and DSC analysis, respectively. Surface free energy analysis indicates the presence of hydrophobic (siloxane) groups on the surface, giving highly hydrophobic nature to the obtained PURs films. Water absorption measurements showed that the increase of the hydrophobic PPO-PDMS segment content led to the decrease of percentage of absorbed water in copolymers. SEM and AFM analysis revealed that copolymers with lower content of PPO-PDMS segments have higher microphase separation between segments. The results obtained in this work indicate that synthesized PURs based on PPO-PDMS demonstrated proper surface and morphological properties with a great potential for variety of applications such as hydrophobic coatings in biomedicine.

Keywords: segmented polyurethanes, poly(dimethylsiloxane), 2D-NMR spectroscopy, surface free energy, morphology.

Available online at the Journal website: http://www.ache.org.rs/HI/

SCIENTIFIC PAPER

UDC 678.664:678–13:543

Hem. Ind. **70** (6) 725–738 (2016)

doi: 10.2298/HEMIND151127009S

Segmented thermoplastic polyurethane elastomers (PURs) are multiblock copolymers consisting of alternating hard (HS) and soft segments (SS). The diversity of PURs and their widespread application arises from the possibility of achieving various compositions of PURs by simple changing their chemical structure and molecular weight of HS and SS segments and/or preparation conditions. In this manner, different properties of the PURs can be easily modified and adopted for specific application, such as coatings for specific purposes. Furthermore, the thermodynamic incompatibility between HS and SS segments leads to the formation of phase-separated micro-domain morphology within the PURs. The morphology of the PURs is one of the main factors that determine their interesting physical and chemical properties. The appearance of phase separation in PURs depends on the composition, nature and length of HS and SS segments [1–3]. According to the Koberstein *et al.* the appropriate length of HS is required for phase separation, and degree of phase separation can be varied with changing in the HS/SS ratio [3].

Constant need for new and enhanced materials led to the application of various macrodiols during the synthesis of PURs, such as polydimethylsiloxane (PDMS). PDMS materials exhibit several outstanding characteristics that enable their widespread use such as low glass transition temperature, great polymer chain flexibility, inertness to high and low temperatures, oxidation resistance, non-toxicity and low surface energy [4–6]. The use of the PDMS segments caused improvement of surface features of PURs and generation of materials with a pronounced hydrophobicity [7,8]. Low surface energy of the PURs and tendency of the PDMS blocks toward surface are the main reasons for achieving greater hydrophobicity and useful surface morphology of the PURs [9]. The surface enrichment with PDMS segments could also efficiently

Correspondence: I.S. Stefanović, Institute of Chemistry, Technology and Metallurgy (ICTM) – Center of Chemistry, University of Belgrade, Njegoševa 12, 11000 Belgrade, Serbia.
E-mail: ivanstefanovic.com8@gmail.com; istefanovic@chem.bg.ac.rs
Paper received: 27 November, 2015
Paper accepted: 10 February, 2016

improve biocompatibility and enhance biostability of PURs in order to use them as waterproof coatings on the various medical devices [10,11].

In recent years, there has been growing interest in preparation of PURs modified with different siloxane based block copolymers, containing various polyether or polyester blocks, in order to obtain PURs with more beneficial features. Recently, the structure-property correlation of PURs based on PDMS was reported in order to apply these PURs as waterproof coatings [12––14]. Furthermore, Martin *et al.* have shown that the use of the PDMS-polyether-mixed macrodiol leads to the formation of PURs with outstanding biostability [15]. Byczyński *et al*. reported PURs coatings, based on different soft segments. With the use of *α,ω*-dihydroxy--terminated PDMS as the SS, they obtained PURs with nonpolar, *i.e*., hydrophobic surface due to the incorporated side-chain siloxane [16]. Moreover, Byczyński *et al*. also prepared novel ecological high-solid poly(urethane-siloxane) networks, based on comb-like structure co-poly(dimethyl)(methyl, 3-glycidoxypropyl)-siloxane, where an increased amount of siloxane resulted in an increase of water contact angle and a decrease of absorbed water as well as surface free energy, that confirmed a significant hydrophobic nature of the employed siloxane [17]. Sheth *et al.* showed that molecular weight of PDMS blocks had a marked effect on the morphology of the obtained polymers [18]. It was demonstrated that copolymers with molecular weights of PDMS blocks of 2500 and especially 7000 g/mol have higher microphase separated structure in comparison to the copolymers based on PDMS of 900 g/mol.

The main goal of this work was to synthesize novel PURs by catalyzed two-step polyaddition process in solution and to investigate the influence of the PPO--PDMS content on the surface properties and morphology of the synthesized PURs. The synthesized PURs are based on 4,4′-methylenediphenyl diisocyanate (MDI) and 1,4-butanediol (BD) as the hard segment and *α,ω*-dihydroxy-poly(propylene oxide)-*b*-poly(dimethylsiloxane)-*b*-poly(propylene oxide) (PPO-PDMS) as the soft segment. The chemical structure of the synthesized PURs and the presence of hydrogen bonds inside polymer chains were investigated by FTIR spectroscopy. The detailed structure and composition of the synthesized PURs were investigated using ^{1}H- and 2D-NMR (COSY, HSQC and HMBC) spectroscopy. Molecular weights and polydispersity index of the synthesized PURs were determined by gel-permeation chromatography (GPC). Crystallinity of the PURs was monitored by differential scanning calorimetry (DSC). Surface and morphological properties of prepared PURs were investigated by contact angle measurements (CA), surface free energy analysis (SFE), water absorption (WA), scanning electron microscopy (SEM) and atomic force microscopy (AFM).

EXPERIMENTAL

Materials

α,ω-Dihydroxy-poly(propylene oxide)-*b*-poly(dimethylsiloxane)-*b*-poly(propylene oxide) (ABCR, purity 95%) was dried over molecular sieves (0.4 nm) before use. The number average molecular weight, M_n, of the PPO-PDMS is determined from ^{1}H-NMR spectroscopy and amounted to 2970 g/mol. Polydispersity index of the PPO-PDMS was determined by GPC analysis and amounted to 1.7. The average degrees of polymerization of the central siloxane block and terminal propylene oxide blocks are 11.9 and 16.5, respectively. 4,4′-Methylenediphenyl diisocyanate (Aldrich, purity 98%), with isocyanate content of 25 wt.%, determined by the standard dibutylamine back-titration method and it was used as received. 1,4-Butanediol (Aldrich, purity 99%) was distilled and dried over molecular sieves before use. *N,N*-Dimethylacetamide (Acros, purity 99%) was dried for 2 h over calcium hydride and distilled under reduced pressure before use. Tetrahydrofuran (J.T. Baker, purity 99.99%) was dried over lithium aluminum hydride and distilled before use. Stannous octoate ($Sn(Oct)_2$; Aldrich, purity 95%), was used as a dilute solution in an anhydrous mixture THF/DMAc (1/1 volume ratio). *N,N*-Dimethylformamide (Macron, purity 99.8%), formamide (Merck, purity 99+%) and diiodomethane (UCB, purity 98%) were used as received.

Synthesis of the PURs

The PURs were synthesized in solution by a catalyzed two-step polyaddition process. The reactants for this reaction were MDI, BD and PPO-PDMS. Series of PURs was consisted of six samples prepared with different content of soft segment (PU-PPO40, PU-PPO50, PU-PPO60, PU-PPO70, PU-PPO80 and PU-PPO90). The last two numbers in the name of the PURs represent the weight percent of the soft segment in copolymers. The molar ratio of the reacting -NCO groups (from MDI) and -OH groups (from BD and PPO-PDMS prepolymer) was 1.1/1. The catalyst for polymerization was stannous octoate (0.15 mol% $Sn(Oct)_2$/PPO-PDMS prepolymer), while a mixture of DMAc/THF (1/1 volume ratio) was used as the solvent mixture.

Polymerization reaction was carried out in a four-neck round-bottom flask equipped with a mechanical stirrer, an inlet for dry argon, a reflux condenser and a dropping funnel. During the synthesis, the flask was placed in a silicone oil bath. Here, the synthesis of the copolymer with mole ratio of PPO-PDMS:MDI:BD = = 1:7:6 (*i.e*., 60 wt.% of PPO-PDMS, for PU-PPO60

sample) is described. The initial reaction mixture was consisted of 8.0 g (2.76 mmol) of PPO-PDMS and 7.2836 g (29.13 mmol) of MDI and 86 mL of solvent mixute DMAc/THF (1/1 volume ratio). The mixure was charged into the flask at room temperature and then heated up to 80 °C under an inert atmosphere. The polymerization started by the introduction of 0.27 mL of catalyst solution in DMAc/THF (1.68 mg, 4.1×10^{-3} mmol). The first phase of the polymerization was carried out at 80 °C for 40 min under continuous stirring, to prepare the NCO-terminated prepolymer, *i.e*., until the theoretical -NCO content was attained. The change in the -NCO content during the polymerization was monitored using the standard dibutylamine back-titration method [19]. In the second stage of the polymerization, the chain extension was achieved by the addition of dilute solution of BD (1.4897 g, 16.6 mmol) in 8.0 mL of DMAc/THF. Diluted solution of BD was added dropwise to the reaction mixture and the second phase of polymerization was continued for 10 h at the same temperature. The final polymer concentration was approximately 15 wt.%. After the polymerization, the reaction mixture was cooled down to the room temperature and the copolymer was precipitated into a methanol/water (1/1 volume ratio) solution. After precipitation, copolymer was washed with methanol several times, filtered and dried in a vacuum oven at 40 °C for 48 h until the constant weight. The yield of this copolymer was 94% while the yields of all synthesized copolymers were in the range from 65 to 95% (Table 1).

Preparation of the PURs films

The films were prepared by dissolving the copolymers in DMF at an elevated temperature and pouring the PURs solution (10 wt.%) into a Teflon® dish (diameter 5 cm) and drying at 40 °C in a force-draft oven for 24 h. The films (typically about 0.3-0.5 mm thick) were then dried under vacuum at 40 °C for 24 h and stored in desiccators at room temperature for two weeks before the characterization.

Characterization

FTIR spectra of the synthesized PURs were recorded using attenuated total reflection (ATR) mode on a Nicolet 6700 FTIR spectrometer. Based on the device characteristics, the scanning range was from 400 to 4000 cm^{-1} at the resolution of 2 cm^{-1} and 64 scans.

NMR experiments were performed on Bruker Avance 500 spectrometer equipped with 5 mm inverse detection *z*-gradient probe. The ^{1}H- and quantitative ^{13}C-NMR spectra (at 500.13 and 125.75 MHz, respectively) were measured at 25 °C using d_6-DMSO as the solvent. Chemical shifts are given on the δ scale relative to the d_6-DMSO signal. The 2D-NMR experiments (COSY, HSQC and HMBC) were performed on standard Bruker pulse sequences. COSY spectrum was collected with four scans per 256 increments, while HSQC and HMBC were collected with eight and sixteen scans per 512 increments, respectively.

The composition*, i.e*., the mole and weight content of SS, was calculated according to the ^{1}H-NMR spectra as the relative intensities of the methyl proton signals arising from the $–SiCH_3$ groups and the terminal $–CH_2$ protons from the BD residues [20]. The mole and weight fractions of the SS were calculated using the following equations:

$$x_{SS} = \frac{\frac{I(SiCH_3)}{6\overline{X_n}+6}}{\frac{I(SiCH_3)}{6\overline{X_n}+6}+\frac{I(CH_2)}{4}} \quad (1)$$

$$w_{SS} = \frac{x_{SS}M_{SS}}{x_{SS}M_{SS}+x_{HS}M_{HS}} \quad (2)$$

where, x_{SS} and x_{HS} are the mole fractions of the soft and hard segments, w_{SS} is the weight fraction of the soft segments, M_{SS} = 3220 g/mol is molecular weight of the soft segment, *i.e*., MDI-PPO-PDMS, M_{HS} = 340 g/mol is molecular weight of the MDI-BD unit and $\overline{X_n}$ = = 11.9 is the degree of polymerization of the PDMS--block in the PPO-PDMS prepolymer.

Table 1. Composition of the reaction mixture, the lenght of the hard segments, L_n(HS), and yields of the synthesized PURs

Sample	Mole ratio[a]	SS, wt.% (in feed)[b]	SS, wt.% (NMR)[c]	SS, mol.% (in feed)[b]	SS, mol.% (NMR)[c]	L_n / HS (NMR)[d]	Yield, %
PU-PPO90	1:2:1	90.3	88.5	50.0	45.5	1.46	65
PU-PPO80	1:3:2	82.0	77.8	33.3	27.5	1.52	89
PU-PPO70	1:5:4	69.8	65.8	20.0	17.2	2.23	90
PU-PPO60	1:7:6	61.1	60.3	14.3	14.1	3.22	94
PU-PPO50	1:11:10	47.8	47.9	9.1	9.0	3.28	95
PU-PPO40	1:15:14	39.1	38.5	6.7	6.3	3.78	87

[a]PPO-PDMS:MDI:BD in the reaction mixture at a 1.1/1 mole ratio of NCO/OH groups; [b]predetermined by the composition of the reaction mixtures; [c]determined by ^{1}H-NMR spectroscopy; [d]determined by quantitative ^{13}C-NMR spectroscopy

A Waters 1525 GPC system (Waters, Milford, MA), consisting of two Styragel columns (HR 1 and HR-5E columns, 4.6 mm×300 mm each, Waters, Milford, MA) connected in series, a binary HPLC pump, a Waters 717 plus autosampler, a Waters 2414 refractive index detector and BreezeTM software, was used to compute molecular weights and molecular weight distribution of the synthesized copolymers. Sample solutions of the copolymers in THF at a concentration of 10 mg/mL were filtered through a 0.45 μm hydrophobic fluoropore (PTFE) filter (Millipore Corporation, Bedford, USA) before injection into the GPC system and eluted with THF at 40 °C, at a flow rate of 0.3 mL/min. The system was calibrated with a number of polystyrene standards ranging from 3680 to 570000 g/mol.

Differential scanning calorimetry was carried out on Q1000V9.0 Build 275 thermal analyzer. The DSC scans were recorded under a dynamic nitrogen atmosphere with flow rate of 50 mL/min. The temperature range of recording was between –90 and 230 °C at a heating and a cooling rate of 10 and 5 °C/min, respectively. The weight of the samples was approximately 10 mg.

Static contact angle of the synthesized PURs was measured by a sessile drop method at 27 °C, using a contact angle analyzer (Krüss DSA100). Surface energy data were calculated from the contact angle values obtained using distilled water, formamide and diiodomethane and the acid-base theory for solids according to the van Oss–Chaudhury–Good approach [21]. Single drops of tested liquid with a volume of 20 μL were deposited on the film surface and the contact angles were measured immediately. Contact angles for each copolymer were calculated as the average value of three measurements.

The surface free energy was calculated using the acid-base theory for solids, according to the van Oss–Chaudhury–Good approach using distilled water, formamide and diiodomethane as liquids for contact angles measurements. From the measured values of contact angles of these liquids in contact with surface of the PURs copolymers, the surface free energy and its components were calculated using the following equations [21]:

$$\gamma_{LV1}\left(1+cos\theta_1\right)=2\sqrt{\gamma_S^{LW}\gamma_{LV1}^{LW}}+\sqrt{\gamma_S^{+}\gamma_{LV1}^{-}}+\sqrt{\gamma_S^{-}\gamma_{LV1}^{+}} \quad (3)$$

$$\gamma_{LV2}\left(1+cos\theta_2\right)=2\sqrt{\gamma_S^{LW}\gamma_{LV2}^{LW}}+\sqrt{\gamma_S^{+}\gamma_{LV2}^{-}}+\sqrt{\gamma_S^{-}\gamma_{LV2}^{+}} \quad (4)$$

$$\gamma_{LV3}\left(1+cos\theta_3\right)=2\sqrt{\gamma_S^{LW}\gamma_{LV3}^{LW}}+\sqrt{\gamma_S^{+}\gamma_{LV3}^{-}}+\sqrt{\gamma_S^{-}\gamma_{LV3}^{+}} \quad (5)$$

$$\gamma_S=\gamma_S^{LW}+\gamma_S^{AB}=\gamma_S^{LW}+2\sqrt{\gamma_S^{+}\gamma_S^{-}} \quad (6)$$

where LW means the Lifshitz-van der Waals interaction, AB means the acid-base interaction, γ_s is the surface free energy contributed by Lifshitz-van der Waals, γ^{LW} is dispersive component, γ^{AB} is polar component, *i.e*., acid-base interaction, γ^{+} and γ^{-} are the Lewis acid parameter and the Lewis base parameter of the surface free energy, respectively, and γ_{LV} is the surface tension of the liquid in equilibrium with its own vapor.

The subscript numbers 1–3 in Eqs. (3)–(5) refer to the various liquids: 1 for distilled water, 2 for formamide and 3 for diiodomethane. According to the literature, it is well known that for van Oss–Chaudhury––Good calculations, the surface tension values for distilled water, formamide and diiodomethane are as those presented in Table 2.

Table 2. surface tension values (mJ/m^2) for distilled water, formamide and diiodomethane [22]

Value	Liquid		
	Water	Formamide	Diiodomethane
γ_{LV}	72.8	58.0	50.8
γ_{LV}^{LW}	21.8	39.0	50.8
γ_{LV}^{-}	25.5	39.6	0
γ_{LV}^{+}	25.5	2.28	0

With the data in Table 2 the total surface energy (γ_S) and its components (γ_S^{LW}, γ_S^{AB}) can be easily calculated by solving the Eq. (6).

Water absorption was investigated at room temperature by sample immersion in phosphate buffered saline (PBS, pH 7.4) at 37 °C, for 1, 3, 5, 7, 24, 28 and 48 h. At each time point, the samples were removed and blotted with filter paper to remove excess of water. The average value of three measurements for each sample was used. The weight percent of the water absorption was calculated according to the following equation:

$$WA = 100\frac{w_W - w_{W0}}{w_{W0}} \quad (7)$$

where w_w is the weight of the fully hydrated sample and w_{W0} is the weight of the dried sample.

The cross-section surface morphology was analyzed by field emission scanning electron microscopy (SEM). Micrographs were obtained on JEOL JSM-6460LV instrument, at a working distance of *ca.* 14 mm and an accelerating voltage of 20 kV. The copolymers were cryo-fractured in liquid nitrogen and coated with a thin layer of gold prior to the measurements.

AFM images were detected on atomic force microscope (Dimension Icon, Bruker, Santa Barbara, CA, USA), equipped with the SSS-NCL probe, Super Sharp Silicon™-SPM-Sensor (NanoSensors™ Switzerland; spring constant 35 N/m, resonant frequency ~170 kHz). Measurements were performed under ambient conditions using the tapping mode AFM technique. The scans area is 50×50 μm^2. The AFM images of the frac-

ture areas of PURs films after previous freeze-fracturing at the temperature of liquid were measured in order to evaluate the inner arrangement in the bulk system.

RESULTS AND DISCUSSION

A series of novel PURs was synthesized using *α,ω*-dihydroxy-poly(propylene oxide)-*b*-poly(dimethylsiloxane)-*b*-poly(propylene oxide) as the soft segment and 4,4′-methylenediphenyl diisocyanate and 1,4-butanediol as the hard segment. The chemical structure of the obtained PURs is shown in Figure 1.

The polymerization was carried out in a solution of two solvents that differ in terms of polarity, THF and DMAc. Combination of these solvents proved to be the best option necessary to ensure good solubility of the reactants and to increase their mutually reactivity [23]. Namely, the applied solvent mixture was chosen according to the criteria that consider improvement of the solubility of dissimilar polymers (polysiloxane and polyurethane) by using solvents, which solubility parameters are close to the solubility parameters of polymers. The solubility parameters of the polymers are $\delta_{PURs} \approx 11.3$ $(cal/cm^3)^{1/2}$ and $\delta_{PDMS} \approx 6.1$ $(cal/cm^3)^{1/2}$, while for solvents they are $\delta_{DMAc} \approx 14.3$ $(cal/cm^3)^{1/2}$ and $\delta_{THF} \approx 8.7$ $(cal/cm^3)^{1/2}$ [24]. The content of SS of the synthesized PURs was changed from from 40 to 90 wt.% in order to investigate the influence of SS content on the surface performances and morphology of the synthesized PURs. The molar ratio of PPO-PDMS prepolymer, MDI and BD, predetermined by the composition of the reaction mixture, was varied from 1:2:1 to 1:15:14 (Table 1). The mole ratio of the –NCO groups and –OH groups in PURs was 1.1/1. The variation in composition of the reaction mixture was used to ensure formation of the desired copolymers content, while the excess of the –NCO groups was used to ensure appropriate degree of polymerization of the synthesized PURs. Different HS/SS ratio was used in this work in order to examine this variation on structure, surface performances and morphology. Incorporation of PPO-PDMS prepolymer as SS, in this type of polyurethanes, lead to significant alterations in surface related properties. These PURs based on siloxane can be used for various applications and one of the most significant is certainly as water resistant coatings on different medical implants [25].

The chemical structure of the synthesized PURs and the presence of hydrogen bonds inside polymer chains were investigated by FTIR spectroscopy. In the Figure 2a), FTIR spectra of some PURs are given. The positions of all absorption bands of different groups were similar for all synthesized PURs. In the FTIR spectra of PURs, absorption bands characteristic for stretching vibrations of the amide II and amide III groups (1535 and 1230 cm^{-1}, respectively), overlapped bands of stretching vibrations of Si–O–Si and C–O–C groups (1020 and 1100 cm^{-1}, respectively) symmetric and asymmetric stretching vibrations of $–CH_2–$ and $–CH_3$ groups (2870

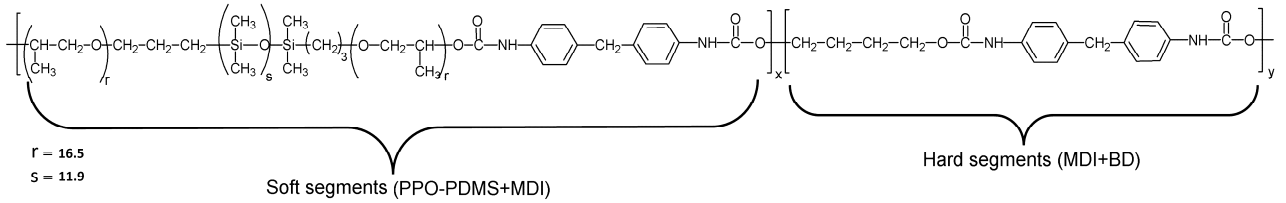

Figure 1. Chemical structure of the PURs composed of hard and soft segments.

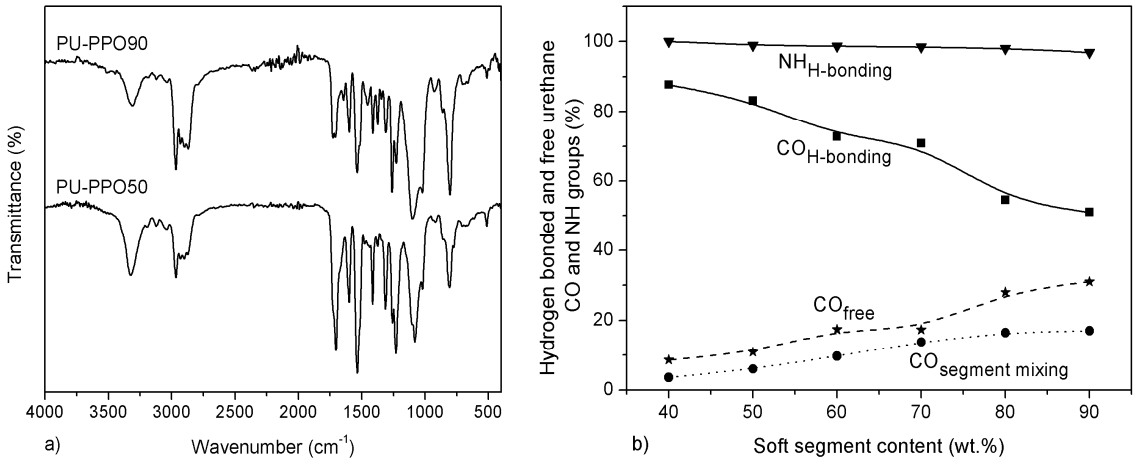

Figure 2. FTIR spectra (a) of the selected PURs and fractions of hydrogen bonded and free C=O and –NH groups as a function of the soft segment content (b), obtained from deconvolution technique.

and 2965 cm^{-1}, respectively), aromatic bands (1415 and 1600 cm^{-1}) and rocking vibrations of the $SiCH_3$ groups (805 cm^{-1}) can be observed.

Moreover, in order to study the influence of the hard segment content on the formation of hydrogen bonds, carbonyl absorption bands (1705 cm^{-1}) and –NH absorption bands (3320 cm^{-1}) were examined in details. The C=O and –NH bands were fitted by a Gaussian deconvolution technique, and the synthesized PURs exhibit three absorbance peaks in the C=O region (hydrogen-bonded carbonyl groups in the ordered and disordered hard domains and free carbonyl groups) and two absorbance peaks in the –NH region (hydrogen-bonded and free –NH groups). Results obtained from Gaussian deconvolution technique are presented in Figure 2b. The deconvolution technique shows that the fraction of hydrogen bonded –NH groups increases with increasing hard segment content, and that almost all urethane –NH groups are involved in hydrogen bonding. Results obtained by deconvolution of the C=O region show that fraction of hydrogen bonded C=O increases, while the fraction of free C=O decreases with increasing hard segment content in PURs. Furthermore, the fraction of hydrogen bonded C=O groups in disordered domains decreases with increasing content of hard segments. The FTIR analysis of the C=O and –NH regions shows that tendency of hydrogen bonding between hard segments is higher in copolymers with lower PPO-PDMS content. This behavior results in certain ordering of hard segment domains, indicating higher degree of phase separation in copolymers with higher content of hard segments. These results are in accordance with literature [26] and SEM and AFM analysis presented below.

The structure of the synthesized PURs was also investigated and confirmed by ^{1}H-NMR spectroscopy. The chemical structure and appropriate assignment of peaks in the ^{1}H-NMR spectrum for copolymer with 70 wt.% of SS (PU-PPO70) are presented in Figure 3.

The mole and weight contents of SS were calculated from ^{1}H-NMR spectra and presented in Table 1. It is shown that the theoretical mole and weight contents of the SS in the PURs are in the range from 6.7 to 50.0 mol.% and from 39.1 to 90.3 wt.%, respectively. While the experimental mole and weight values calculated from ^{1}H-NMR are in the range from 6.3 to 45.5 mol.% and from 38.5 to 88.5 wt.%. It is noticeable that slightly larger deviations from the set point values are obtained for the PURs with the highest SS content. This probably occurred because these copolymers have slightly lower degree of conversion and therefore the second phase of reaction should be carried out for a longer time. Results summarized in Table 1 indicate that the obtained compositions of the PURs are mainly in accordance with the set theoretical values and that by using the synthetic procedure described in this work it is possible to vary and adjust the composition of final PURs for some specific desirable application.

The lengths of the hard segments, L_n(HS), were calculated from the quantitative ^{13}C-NMR spectroscopy results. L_n(HS) is defined as the number of repeating MDI-BD units per one SS. From the quantitative ^{13}C--NMR spectrum, which is part of the HMBC spectrum, it can be seen that signal from aromatic carbons con-

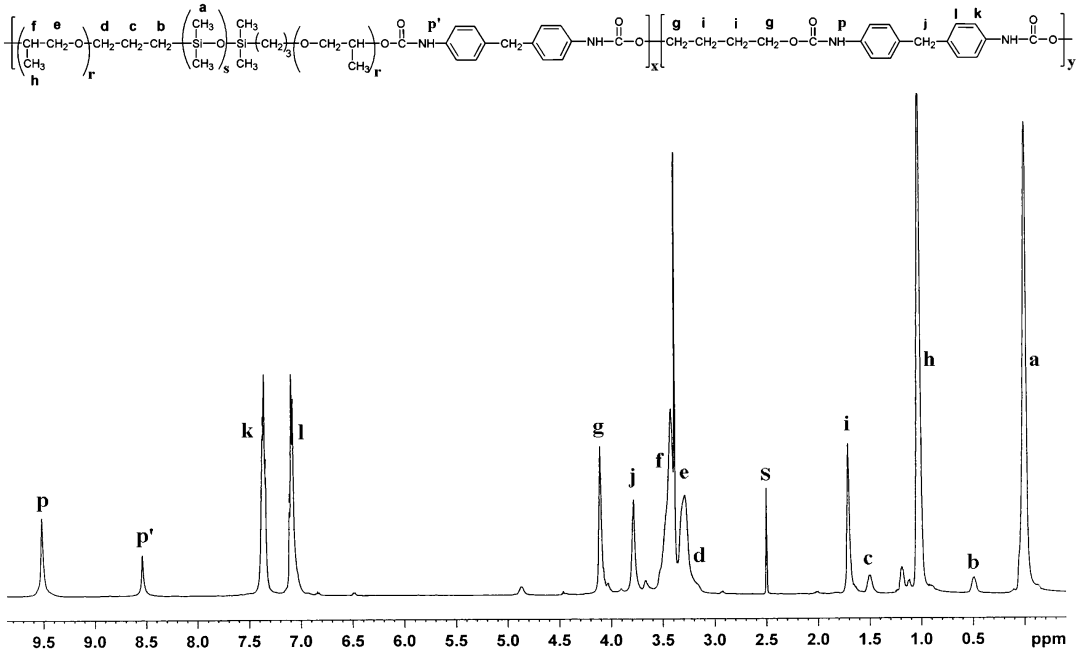

Figure 3. ^{1}H-NMR spectra of the synthesized copolymer with 70 wt.% of the PPO-PDMS.

tained in MDI are splitted into two different signals (m' and m at ~134 and 135 ppm and n and n' at ~137 and 138 ppm). This is the result of the existence of two different bonds [20], bonds between MDI and BD and between MDI and PPO-PDMS parts. The experimental values of L_n(HS) were calculated from quantitative ^{13}C-NMR spectra using the following formula:

$$L_n(\text{HS}) = I(\text{m})/I(\text{m}') \quad (8)$$

where I(m) is integral of aromatic carbon signal from MDI that is connected to BD, while I(m') is integral of aromatic carbon signal from MDI connected to PPO--PDMS.

The obtained average values of L_n(HS) in copolymers are in the range from 1.46 to 3.78, while the theoretical values from 1 to 14, according to the composition of the feed. The obtained values of L_n(HS) are presented in Table 1 and they increased with increasing content of HS in copolymers. The reason for this deviation and for not achieving higher L_n(HS) values, might be the polydispersity of the PPO-PDMS prepolymer and formation of polydisperse NCO-prepolymer in the first stage of the polyaddition reaction [27]. The polydispersity of prepolymer and NCO-prepolymer has the main influence on the disorganization in polymer chains and for the inability to achieve setpoints for the higher lengths of the HS.

In addition, the structure of the synthesized multiblock copolymers was also investigated in detail and confirmed by 2D-NMR spectroscopy. The assignments of the carbon and proton resonances, as well as COSY, HSQC and HMBC spectra, of PU-PPO60, are presented in Figures 4 and 5. 2D-NMR spectra were used to determine the chemical shifts that were missing and/or barely visible (such as *f, e* and *d* protons in Figure 3) in the ^{1}H- and ^{13}C-NMR spectra. To our best knowledge, there is no published study that investigated the structure of these copolymers by 2D-NMR spectroscopy in details. Moreover, the assignments of the proton and carbon resonances within the structures, which belong to the aromatic protons and carbons, the carbonyl carbons and urethane –NH protons in HS and SS, were resolved by COSY, HSQC and HMBC experiments.

In the COSY spectrum, the most expected correlations between neighboring protons, such as Hb-Hc, Hc-Hd and Hh-Hf are shown and clearly visible. Moreover, these correlations also include interactions between protons from BD residues Hi-Hg and interactions from aromatic protons from MDI residues Hk-Hl.

In the ^{1}H-NMR spectrum it can be observed that protons derived from methylene and methine groups from propylene oxide residues and terminal protons from the PPO-PDMS propyl group are overlapped and have similar chemical shifts between 3.2–3.5 ppm. These overlapped *f, e* and *d* signals in the ^{1}H-NMR spectrum were resolved and splitted using HSQC correlations. According to the HSQC spectrum (Figure 4), the methylene and methine groups from propylene oxide residues are located at 3.39 and 3.43 ppm, respectively, while the signal for terminal protons from the PPO--PDMS propyl group is located at 3.28 ppm. Furthermore, in HSQC spectrum other correlations between related carbons and protons are also marked and clearly visible in Figure 4. Correlations from carbons and protons from methyl and methylene groups from PDMS block are labeled as Ca-Ha, Cb-Hb and Cc-Hc signals, respectively. Correlation between carbon and proton inside methyl group from propylene oxide residues are marked as Ch-Hh signal. Moreover, correlations between central and terminal carbons and pro-

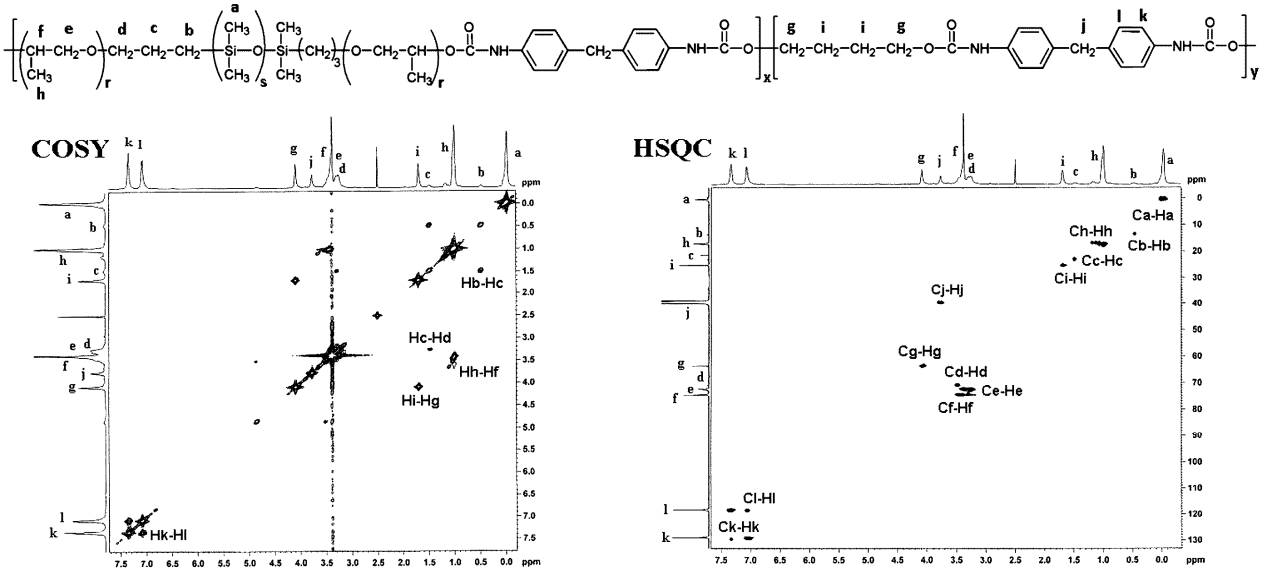

Figure 4. COSY and HSQC spectra of the PURs copolymer with 60 wt.% of the PPO-PDMS.

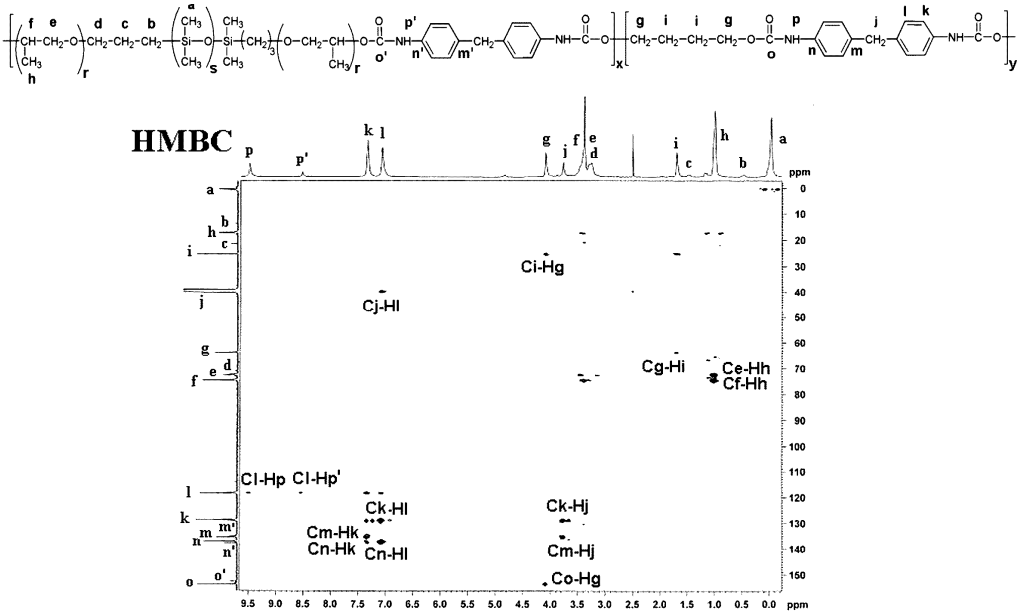

Figure 5. HMBC spectrum of the PURs copolymer with 60 wt.% of the PPO-PDMS.

tons inside methylene groups from the BD residues, are designated as Ci-Hi, Cg-Hg signals, respectively, while correlations inside and between aromatic rings are labeled as Cl-Hl, Ck-Hk and Cj-Hj signals.

In HMBC spectrum (Figure 5), certain correlations between carbons and protons that exist between distant (multiple-bond) hetero nuclei can be observed. The urethane –NH protons from the HS and SS were identified by HMBC based on Cl-Hp and Cl-Hp' correlations (signals that are labeled with ' refer to the SS protons), which indicates that MDI moieties are incorporated into the both, HS and SS, of the synthesized PURs. The signal of urethane –NH protons of the HS appears at 9.50 ppm, while the position of the signal of urethane –NH protons from the SS appears at 8.54 ppm. The urethane carbonyl atom from the HS, which appears at δ = 153.65 ppm, bonded to the BD moiety, showed HMBC correlations Co-Hg. From these results it follows that signal of carbonyl urethane group –NH**C**OO–, which is connected to the PPO-PDMS segment (from SS), was observed at δ = 152.61 ppm. That also confirms that –NHCOO– groups can be equally formed by the reaction between MDI with BD and between MDI and PPO-PDMS segments. In HMBC spectrum, other correlations between multiple bonded hetero-nuclei are also labeled and clearly visible in Figure 5. Correlations that exist between methylene and methine carbons and protons from methyl groups inside propylene oxide residues are marked as Ce-Hh and Cf-Hh signals. Correlations between distant central and terminal carbons and protons inside BD residues, are designated as Cg-Hi, *i.e.*, Ci-Hg signals. Moreover, correlations that apear between distant carbons and protons inside aromatic rings from the MDI, are labeled as Ck-Hj, Ck-Hl, Cm-Hj, Cm-Hk, Cn-Hl, Cn-Hk and Cj-Hl signals.

2D-NMR spectra completely confirm the structure of these copolymers and incorporation of PPO-PDMS blocks as the SS and also incorporation of MDI moieties into both HS and SS.

The molecular weights and molecular weight distribution of the synthesized PURs were determined by gel permeation chromatography. The number (M_n) and weight (M_w) average molecular weights and polydispersity index (*PDI*) of PURs are reported in Table 3 and obtained GPC chromatograms are shown in Figure 6.

Table 3. The average molecular weights, M_n and M_w, index polydispesity, PDI, and the degree of crystallinity of the synthesized PURs

Sample	$M_n\times10^{-3}$ g/mol	$M_w\times10^{-3}$ g/mol	*PDI*	X_c[a] %	X_c^{HSa} %
PU-PPO90	10.6	31.0	2.9	–	–
PU-PPO80	34.1	40.6	1.2	–	–
PU-PPO70	14.6	41.8	2.9	–	–
PU-PPO60	47.1	76.5	1.6	2.2	5.5
PU-PPO50	45.2	52.7	1.2	2.4	4.6
PU-PPO40	32.9	36.8	1.1	8.2	13.3

[a]Determined by DSC analysis

From the obtained results it can be observed that M_n of the synthesized PURs is between 10.6 and 47.1×10^3 g/mol, while the polydispersity index is in the range from 1.1 to 2.9. The weight average molecular weights are in the range from 31.0 to 76.5×10^3 g/mol. The values of molecular weights varied with changes in the copolymers composition. The highest values of M_n

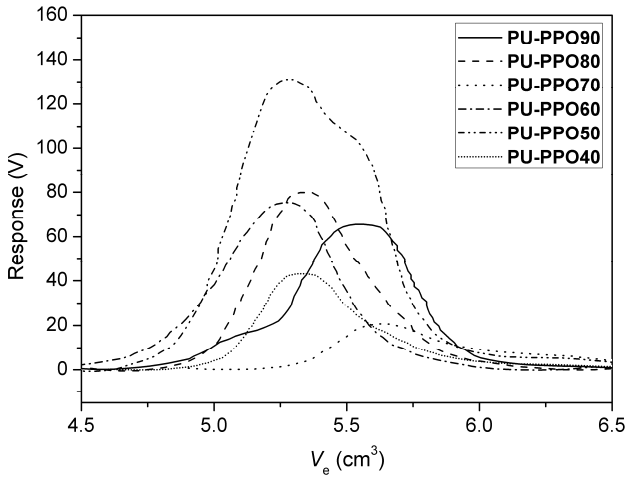

Figure 6. GPC chromatograms of the synthesized PURs.

and M_w were obtained for the PU-PPO60 copolymer. According to these results it seems that the copolymer with 60 wt.% of SS represents the boundary for reaching the highest molecular weights, under these reaction conditions.

From Figure 6 it can be seen that copolymers PU--PPO80, PU-PPO60 and PU-PPO40 have unimodal molecular weight distribution, while other PURs have small shoulder due to the presence of low-molecular weight oligomers. The main reason for this might be the polydispersity of the PPO-PDMS prepolymer and probably formation of polydisperse NCO-prepolymer in the first phase of the reaction [27]. Therefore, appearance of the shoulder in some synthesized copolymers indicates the presence of nonuniform distribution of the molecular weights and higher *PDI* values. To prepare PURs with higher molecular weights, the preparation condition should be more controlled with required variations and perhaps it is necessary that chain extension be more efficient.

The crystallinity of the synthesized copolymers was determined by DSC analysis. The total degrees of crystallinity (X_c) and degrees of crystallinity of the hard segments (X_c^{HS}) were calculated by following equations:

$$X_c = \Delta H_m / \Delta H_m^{\Theta} \quad (9)$$

$$X_c^{HS} = X_c / w_{HS} \quad (10)$$

where w_{HS} is the weight fraction of hard segments determined by ^{1}H-NMR spectroscopy, ΔH_m is the enthalpy of the melting of PUR copolymers and ΔH_m^{Θ} is the enthalpy of the melting of the perfectly crystalline MDI-BD homopolymer, calculated based on the group contributed method (ΔH_m^{Θ} = 91.2 J/g) [28].

The X_c and X_c^{HS} values varied between 2.2 and 8.2% and 5.5 and 13.3%, respectively (Table 3), and they increased with decreasing content of SS. The X_c and X_c^{HS} values were not calculated for copolymers with low content of hard segments due to the fact that they have short length and could not crystallize. Due to the absence of any crystallinity, these copolymers are considered to be amorphous. These results indicate that synthesized PURs are partly crystalline polymers with small crystallinity degree, which is a consequence of the short length of the hard segments. Similar results have been reported by Dai *et al*. [29].

The contact angles determined for the synthesized PURs in contact with distilled water are in the range from 89.0 to 103.3° (Table 4), clearly indicating the hydrophobic surface of the invesigated samples. The contact angles with formamide and diiodomethane are in the range from 78.2 to 91.5° and 72.3 to 76.6°, respectively (Table 4). It is observed from Table 3 that copolymer PU-PPO90 has the highest values of water, formamide and diiodomethane contact angles and that with decreasing SS content, these values of contact angles decreases as well. From the obtained results, it was concluded that incorporation of the PPO-PDMS segments significantly increases the water contact angle, making the surface more hydrophobic. Interestingly, the obtained results for contact angles are higher than values measured for our previously reported siloxane–urethane copolymers based on *ε*-caprolactone-PDMS, ethylene oxide-PDMS and hydroxy propyl-PDMS [27,30,31]. The reason for achieving higher values might be due to easier migration of PDMS blocks on the surface of the films and due to the presence of poly(propylene oxide) blocks, which can also enhance the hydrophobicity of the PURs films.

The obtained results for surface free energy showed that the dispersive (y_S^{LW}) components increased, while the polar (y_S^{AB}) components showed no specific trend with decreasing PPO-PDMS content. The dispersive and polar components have values in the range from 19.30 to 21.62 mJ/m^2 and between 2.29 and 6.05 mJ/m^2, respectively. It is evident that dispersive components

Table 4. Static water contact angle (θ_1), formamide contact angle (θ_2), diiodomethane contact angle (θ_3), surface free energy and its components and R_q values of the synthesized PURs

Sample	θ_1[a] / °	θ_2[a] / °	θ_3[a] / °	γ_S^{LW}	γ_S^+	γ_S^-	γ_S^{AB}	γ_S	R_q / nm
PU-PPO90	103.3±0.6	91.5±3.0	76.6±0.9	19.30	0.36	12.76	4.29	23.58	91.8
PU-PPO80	100.0±2.1	88.0±0.8	75.0±0.6	20.12	0.11	15.57	2.62	22.74	150.0
PU-PPO70	97.9±0.9	86.7±0.6	73.8±0.4	20.80	0.11	18.77	2.92	23.72	288.0
PU-PPO60	97.0±1.7	86.0±2.9	73.9±0.9	20.72	0.07	20.26	2.29	23.01	131.0
PU-PPO50	93.0±1.8	84.4±3.8	72.9±0.1	21.27	0.12	29.98	3.84	25.10	702.0
PU-PPO40	89.0±1.5	78.2±1.7	72.3±1.1	21.62	0.30	30.42	6.05	27.68	90.1

[a]Values are expressed as mean ± standard error

are much higher than the polar components, indicating on significant intermolecular attractions between polymer chains. Electron-acceptor interaction, γ_S^+, are in the range from 0.07 to 0.36 mJ/m^2, while the electron-donor interactions, γ_S^-, are in the range from 12.76 to 30.42 mJ/m^2. The contribution of electron-acceptor interaction to the total polar components interactions, γ_S^{AB}, is low in comparison to the contribution from the electron-donor interactions. The obtained results revealed that surface free energy of the copolymers decreased with increasing PPO-PDMS content in the synthesized PURs, due to the surface activity of hydrophobic PPO-PDMS incorporated as soft segment. The values of the surface energy of the synthesized copolymers were in the range from 22.74 to 27.68 mJ/m^2 and were slightly higher than values obtained for the siloxane–urethanes reported in the literature (approximately 20 mJ/m^2) [16,32] and silicone control sample (18 mJ/m^2) [32]. Such behavior is partly because the PPO-PDMS covers mainly the entire PURs surface and partly because of the surface activity of the PPO-PDMS. To sum up, the obtained results indicate the presence of the hydrophobic siloxane groups at the surface, resulting in highly hidrophobic nature of synthesized PURs. Obtained results are in a good agreement with the results published by Gradinaru *et al.* [10].

The water resistance of the synthesized copolymers was investigated by simple water absorption testing (Figure 7). Results show that the weight percentages of the absorbed water reached an equilibrium after 7 h of immersion and those values are between 1.08 and 1.63%. The values for water absorption after 24, 28 and 48 h have not significantly changed after reaching maximum of absorbed water after 7 h with the exception for the copolymer PU-PPO70, where is a slightly larger amount of absorbed water. Furthermore, resluts presented in Figure 7 also show that the weight percentage of water absorption noticeably decreases with increasing in PPO-PDMS content in the synthesized copolymers.

The water absorption values are quite low, indicating that these copolymers are highly hydrophobic. Such surface hydrophobicity is based on extremely hydrophobic nature and low surface energy of PPO-PDMS. Because of these facts, PPO-PDMS has the ability to migrate and cover the surface of the PURs films, thus ensuring hydrophobic nature of these copolymers. It is also well known that methyl groups attached to the Si-O bond inside PDMS blocks, are responsible for hydro-

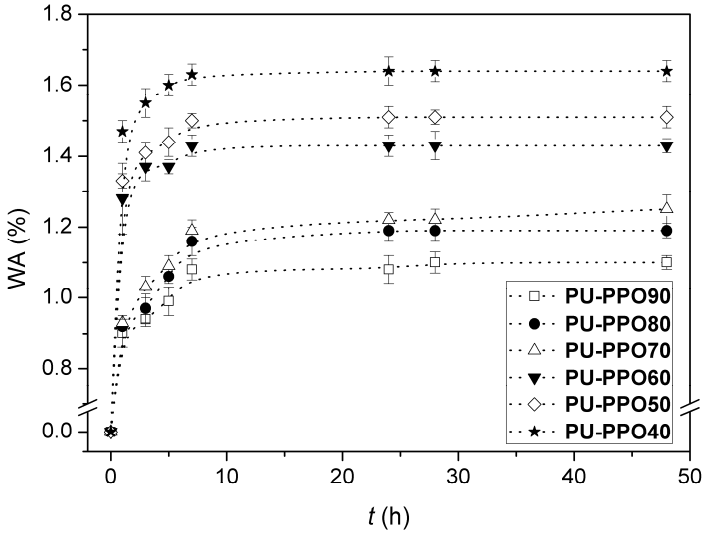

Figure 7. Water absorption of the synthesized PURs vs. time.

phobic character of PPO-PDMS macrodiol [33]. Therefore, these polyurethane copolymers based on PPO-PDMS, exhibit outstanding water resistance, which is one of the most important prerequisite for their possible application as waterproof coatings [6].

Scanning electron microscopy was used to investigate the cross-sectional morphology of the synthesized PURs. The obtained SEM micrographs of PU--PPO90, PU-PPO70 and PU-PPO40 are presented in Figure 8 (a, b and c, respectively). The brighter regions in the cross-section images represent the microdomains of HS, while the darker region represents SS phase. Figure 8 shows a typical view of microdomains of HS which are hydrogen-bonded in small parts, irregular in shapes and unevenly dispersed in the SS phase within the PU-PPO90 copolymer. In the PU-PPO70 and especially PU-PPO40 copolymer SEM micrographs revealed the connection of the hard domains in better organized structure due to the higher presence of hydrogen bonds. Furthermore, connection of the hard domains in these copolymers in comparison to the PU-PPO90 copolymer is also a result of increasing of length of the hard (MDI-BD) segments. SEM analysis was shown good microphase separation that is more pronounced in copolymers with lower content of SS. Observed microphase separation in these PURs has also been confirmed by Dai *et al.* [29].

AFM analysis was used to explore deeper internal and cross-sectional morphology and dispersion of HS within the SS phase of the synthesized PURs. 3D (a, c, e) and 2D phase (b, d, f) images of PU-PPO90, PU-PPO70 and PU-PPO50 copolymers are presented in Figure 9. Root-mean-square, roughness coefficient (R_q) values are summarized in Table 4. According to the literature, the brighter regions represent the HS phase (hard domains or crystalline structures in polyurethane), while the darker regions represent the SS phase [34].

The recorded images revealed that the synthesized copolymers possess two-phase morphology, consisted of the HS and SS phase. It can be observed that copolymers have heterogeneous morphology, which is more pronounced in copolymers with lower SS content due to the present microphase separation between segments. The obtained images indicate that copolymer PU-PPO90 has more uniform structure in comparison to the other copolymers due to the larger SS content. Moreover, it can be clearly noted from the 3D images of copolymers PU-PPO70 and PU-PPO50 that they have much bigger and more noticeable hard segment domains. Phase images show that copolymers with lower content of SS have sharper interface between segments indicating existence of greater microphase separation. Obtained AFM images are in accordance with previous recorded SEM micrographs. Furthermore, it is evident that the cross-sectional (bulk) structure of the copolymers is changed with change in composition and R_q varies in PURs (Table 3). The roughness coefficient is in the range from 90.1 to 702.0 nm and generally increases with decreasing content of SS in the synthesized copolymers. The AFM images also demonstrated that the PURs formed a microphase separated structure which is more pronounced in copolymers with lower SS content.

CONCLUSIONS

The synthesis, surface and morphological properties of PURs prepared with different SS content are described in this work. Series of six new polyurethane copolymers was prepared based on *α*,*ω*-dihydroxy--poly(propylene oxide)-*b*-poly(dimethylsiloxane)-*b*-poly-(propylene oxide) as the soft segment and 4,4′-methylenediphenyl diisocyanate and 1,4-butanediol as the hard segment.

The multiblock structure of PURs was confirmed and examined in details by FTIR, ^{1}H-, ^{13}C-NMR and 2D--NMR (COSY, HSQC and HMBC) spectroscopy. FTIR analysis confirmed strong hydrogen bonds inside hard segments that lead to the formation of microphase separation in copolymers. GPC analysis showed mainly unimodal distribution. DSC analysis revealed that PURs are partly crystalline polymers with small crystallinity,

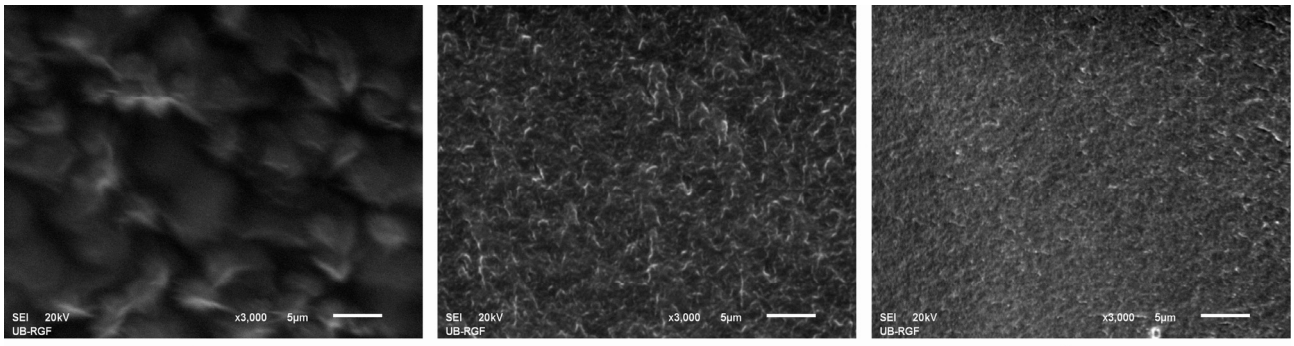

Figure 8. SEM micrographs of the fractured cross-section of the selected PURs containing 90 (a), 70 (b) and 40 wt.% (c) of the soft segments (magnification: 3000×).

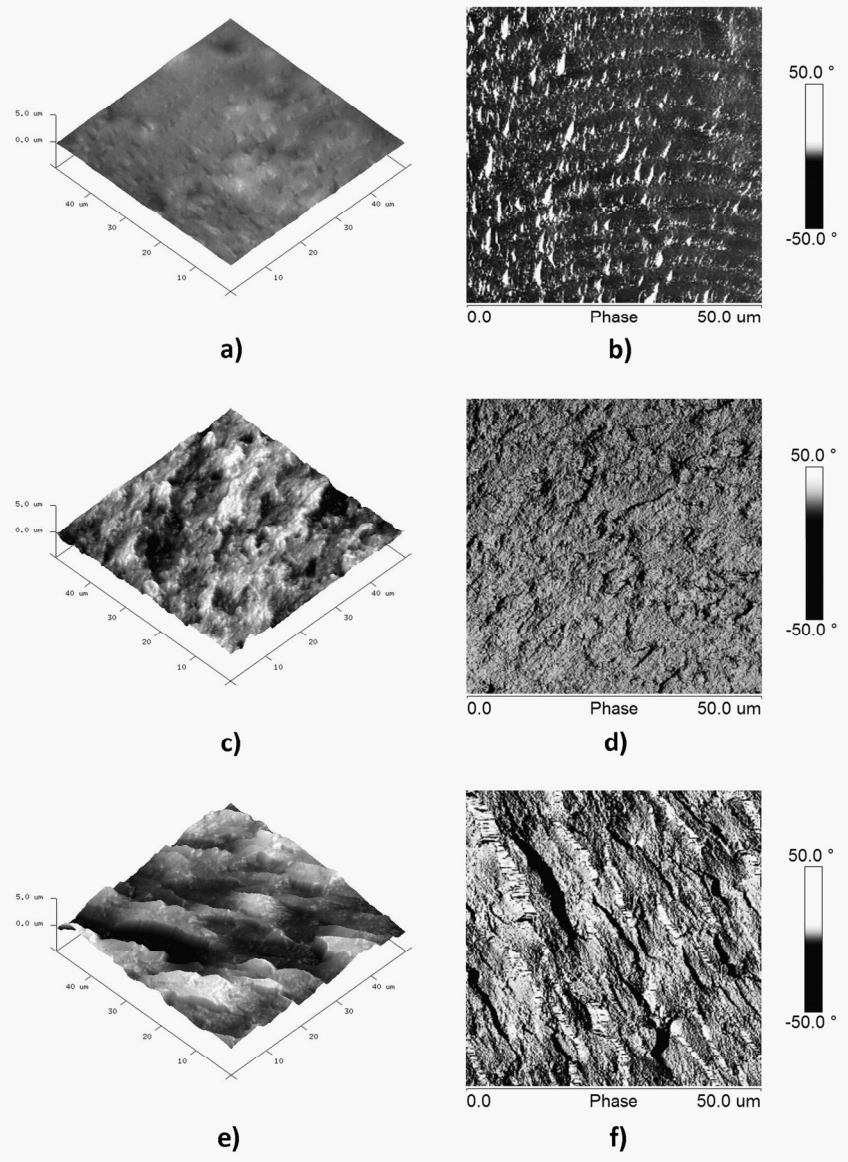

Figure 9. 3D and 2D phase AFM images of the cross-section areas of the selected PURs containing 90 (a, b), 70 (c, d) and 50 wt.% (e, f) of the soft segments (scan size: 50×50 μm^2).

arising from the crystallization of the longer hard segments. Increasing of the water contact angle values and decreasing in surface free energy of the synthesized PURs, with an increase in SS content, clearly indicate the hydrophobic nature of the PURs due to the presence of PDMS blocks within the SS. Furthermore, surface free energy analysis shows the presence of hydrophobic siloxane groups on the surface, giving highly hidrophobic nature to the surface of the synthesized PURs. With increasing content of PPO-PDMS blocks in copolymers, hydrophobicity was increased, due to low surface energy of PPO-PDMS that promotes its migration toward the surface of the synthesized PURs. SEM and AFM analysis revealed existence of microdomains of the HS within the SS phase and that decrease of the SS content led to the higher microphase separation between segments in the synthesized PURs.

The overall results indicate that combination of nonpolar PPO-PDMS and polar MDI-BD segments, utilized to prepare new type of polyurethane copolymers, provided outstanding hydrophobic features. In addition, the incorporation of PPO-PDMS allows modification of the surface and adjustment of morphology of the PURs, which can be used to customize PURs to the requirements necessary for specific applications.

Acknowledgement

This work was financially supported by the Ministry of Education, Science and Technological Development of the Republic of Serbia (Project No. 172062) and by

the Czech Science Foundation (Grant Agency of the Czech Republic, Project No. 13-06700S).

REFERENCES

[1] J.T. Koberstein, R.S. Stein, Small-angle X-ray scattering studies of microdomain structure in segmented polyurethane elastomers, J. Polym. Sci. Polym. Phys. **21** (1983) 1439–1472.

[2] L.M. Leung, J.T. Koberstein, Small-angle scattering analysis of hard-microdomain structure and microphase mixing in polyurethane elasomers, J. Polym. Sci. Polym. Phys. **23** (1985) 1883–1913.

[3] J.T. Koberstein, A.F. Galambos, Multiple melting in segmented polyurethane block copolymers, Macromolecules **25** (1992) 5618–5624.

[4] R. Hernandez, J. Weksler, A. Padsalgikar, J. Runt, Microstructural organization of three-phase polydimethylsiloxane–based segmented polyurethanes, Macromolecules **40** (2007) 5441–5449.

[5] H.D. Hwang, H.J. Kim, Enhanced thermal and surface properties of waterborne UV-curable polycarbonate based polyurethane (meth)acrylate dispersion by incorporation of polydimethylsiloxane, React. Funct. Polym. **71** (2011) 655–665.

[6] Z. Wu, H. Wang, X. Tian, P. Cui, X. Ding, X. Ye, The effects of polydimethylsiloxane on transparent and hydrophobic waterborne polyurethane coatings containing polydimethylsiloxane. Phys. Chem. Chem. Phys. **16** (2014) 6787–6794.

[7] N. Roohpour, J.M. Wasikiewicz, D. Paul, P. Vadgama, I.U. Rehman, Synthesis and characterization of enhanced barrier polyurethane for encapsulation of implantable medical devices, J. Mater. Sci.: Mater. Med. **20** (2009) 1803–1814.

[8] R. Adhikari, P.A. Gunatillake, S.J. McCarthy, G.F. Meijs, Mixed macrodiol-based siloxane polyurethanes: Effect of the comacrodiol structure on properties and morphology, J. Appl. Polym. Sci. **78** (2000) 1071–1082.

[9] M. Rochery, I. Vroman, T.M. Lam, Incorporation of poly(dimethylsiloxane) into poly(tetramethylene oxide) based polyurethanes: The effect of synthesis conditions on polymer properties, J. Macromol. Sci. A. **40** (2003) 321–333.

[10] L.M. Gradinaru, C.Ciobanu, S. Vlad, M. Drobota, M. Butnaru, G. Saint-Pierre, Thermal behavior, surface energy analysis, and hemocompatibility of some polycarbonate urethanes for cardic engineering, High Perform. Polym. **27** (2015) 637–645.

[11] D. Spiller, C. Mirtelli, P. Losi, E. Briganti, S. Sbrana, C. Counoupas, S. Kull, S Tonlorenzi, G. Soldani, *In vitro* evaluation of the PEtU–PDMS material immunocompatibility: The influence of surface topography and PDMS content, J. Mater. Sci.: Mater. Med. **20** (2009) 2511–2520.

[12] S. Awad, H.M. Chen, G.D. Chen, X.H. Gu, J.L. Lee, E.E. Abdel–Hady, Y.C. Jean, Free volumes, glass transition, and cross–links in zinc oxide/waterborne polyurethane nanocomposites, Macromolecules **44** (2011) 29–38.

[13] A. Santiago, L. Martin, J.J. Iruin, M.J. Fernandez-Berridi, A. Gonzalez, L. Irusta, Microphase separation and hydrophobicity of urethane/siloxane copolymers with low siloxane content, Prog. Org. Coat. **77** (2014) 798–802.

[14] F. Yu, X. Xu, N. Lin, H.Y. Liu, Structural engineering of waterborne polyurethane for high performance waterproof coatings, RSC Adv. **5** (2015) 72544–72552.

[15] D.J. Martin, L.A. Poole-Warren, P.A. Gunatillake, S.J. McCarthy, G.F. Meijs, K. Schindhelm, Polydimethylsiloxane/polyether–mixed macrodiol-based polyurethane elastomers: biostability, Biomaterials **21** (2000) 1021–1029.

[16] L. Byczynski, Effect of different polyethers on surface and thermal properties of poly(urethane–siloxane) copolymers modified with side-chain siloxane, J. Therm. Anal. Calorim. **114** (2013) 397–408.

[17] L. Byczynski, M. Dutkiewicz, H. Maciejewski, Synthesis and properties of high-solids hybrid materials obtained from epoxy functional urethanes and siloxanes, Prog. Org. Coat. **84** (2015) 59–69.

[18] J.P. Sheth, A. Aneja, G.L. Wilkes, E. Yilgor, G.E. Atilla, I. Yilgor, F.L. Beyer, Influence of system variables on the morphological and dynamic mechanical behavior of polydimethylsiloxane based segmented polyurethane and polyurea copolymers: a comparative perspective, Polymer **45** (2004) 6919–6932.

[19] A. Marand, J. Dahlin, D. Karlsson, G. Skarping, M. Dalene, Determination of technical grade isocyanates used in the production of polyurethane plastics, J. Environ. Monitor. **6** (2004) 606–614.

[20] M.V. Pergal, I.S. Stefanović, D. Gođevac, V.V. Antić, V. Milačić, S. Ostojić, J. Rogan, J. Djonlagić, Structural, thermal and surface characterization of thermoplastic polyurethanes based on poly(dimethylsiloxane), J. Serb. Chem. Soc. **79** (2014) 843–866.

[21] C.J. van Oss, R.J. Good, M.K. Chaudhury, Additive and nonadditive surface tension components and the interpretation of contact angles, Langmuir **4** (1988) 884–891.

[22] J. Vince, B. Orel, A. Vilčnik, M. Fir, A.V. Šurca, V. Jovanovski, B. Simočič, Structural and water-repellent properties of a urea/poly(dimethylsiloxane) sol–gel hybrid and its bonding to cotton fabric, Langmuir **22** (2006) 6489–6497.

[23] S.L. Rosen, in Fundamental principles of polymeric materials, 2nd ed., C.S. Brazel, S.L. Rosen, Eds., John Wiley and Sons, Inc., New York, 1993, p. 226.

[24] F. Joki-Korpela, T.T. Pakkanen, Incorporation of polydimethylsiloxane into polyurethanes and characterization of copolymers, Eur. Polym. J. **47** (2011) 1694–1708.

[25] E. Briganti, P. Losi, A. Raffi, Silicone based polyurethane materials: a promising biocompatible elastomeric formulation for cardiovascular applications, J. Mater.Sci.: Mater. Med. **17** (2006) 259–266.

[26] T. Choi, J. Weksler, A. Padsalgikar, J. Runt, Microstructural organization of polydimethylsiloxane soft segment polyurethanes derived from a single macrodiol, Polymer **51** (2010) 4375–4382.

[27] M.V. Pergal, V.V. Antic, G. Tovilovic, J. Nestorov, D. Vasiljevic-Radovic, J. Djonlagic, *In Vitro* Biocompatibility

Evaluation of Novel Urethane–Siloxane Co-Polymers Based on Poly(ε-Caprolactone)-block-Poly(Dimethylsiloxane)-block-Poly(ε-Caprolactone), J. Biomat. Sci. Polym. Ed. **23** (2012) 1629–1657.

[28] D.W. Van Krevelen, Properties of Polymers, Elsevier, Amsterdam, 1990.

[29] Z. Dai, K. Yang, Q. Dong, Mechanical, thermal and morphology properties of thermoplastic polyurethane copolymers incorporating *α,ω*-dihydroxy-[poly(propyleneoxide)-poly(dimethylsiloxane)-poly(propyleneoxide)] of varing poly(propyleneoxide) molecular weight, Open J. Synth. Theory Appl. **4** (2015) 41–57.

[30] M.V. Pergal, J. Nestorov, G. Tovilovic, S. Ostojic, D. Goñevac, D. Vasiljevic-Radovic, J. Djonlagic, Structure and properties of thermoplastic polyurethanes based on poly(dimethylsiloxane): assessment of biocompatibility, J. Biomed. Mater. Res. A **102** (2014) 3951–3964.

[31] I.S. Stefanović, J. Djonlagić, G. Tovilović, J. Nestorov, V.V. Antić, S. Ostojić, M.V. Pergal, Poly(urethane-dimethylsiloxane) copolymers displaying a range of soft segment contents, noncytotoxic chemistry, and nonadherent properties toward endothelial cells, J. Biomed. Mater. Res. A **103** (2014) 1459–1475.

[32] P. Majumdar, S. Stafslien, J. Daniels, D. Webster, High throughput combinatorial characterization of thermosetting siloxane–urethane coatings having spontaneously formed microtopographical surfaces, J. Coat. Technol. Res. **4** (2007) 131–138.

[33] H. Jiang, Z. Zheng, W. Song, Z. Li, X. Wang, Alkoxysilane functionalized polyurethane/polysiloxane copolymers: synthesis and the effect of end–capping agent, Polym. Bull. **59** (2007) 53–63.

[34] S. Zhang, Z. Chen, M. Guo, J. Zhao, X. Liu, Waterborne UV-curable polycarbonate polyurethane nanocomposites based on polydimethylsiloxane and colloidal silica with enhanced mechanical and surface properties, RSC Adv. **4** (2014) 30938–30947.

IZVOD

UTICAJ POLI(PROPILEN-OKSID)-*b*-POLI(DIMETILSILOKSAN)-*b*-POLI(PROPILEN-OKSID) MAKRODIOLA NA POVRŠINSKA SVOJSTVA POLIURETANSKIH KOPOLIMERA

Ivan S. Stefanović[1], Dejan Goñevac[1], Milena Špírková[2], Petar Jovančić[3], Vele Tešević[4], Vesna Milačić[5], Marija V. Pergal[1]

[1]*Institut za Hemiju, Tehnologiju i Metalurgiju (IHTM) – Centar za hemiju, Univerzitet u Beogradu, Njegoševa 12, 11000 Beograd, Srbija*
[2]*Institute of Macromolecular Chemistry AS CR, v.v.i. (IMC), Heyrovsky Sq. 2, 16206 Prague 6, Czech Republic*
[3]*Tehnološko–metalurški fakultet, Univerzitet u Beogradu, Karnegijeva 4, 11000 Beograd, Srbija*
[4]*Hemijski fakultet, Univerzitet u Beogradu, Studentski trg 12–16, 11000 Beograd, Srbija*
[5]*North Campus Research Complex, B20, University of Michigan, Ann Arbor, MI 48109, USA*

(Naučni rad)

Poli(uretan-siloksanski) segmentirani kopolimeri (PURs) su sintetisani koristeći 4,4′-metilendifenil-diizocijanat i 1,4-butandiol kao tvrdi segment i *α*,*ω*-dihidroksi--poli(propilen oksid)-*b*-poli(dimetilsiloksan)-*b*-poli(propilen-oksid) (PPO-PDMS) kao meki segment. Sadržaj ugrađenih mekih segmenta u kopolimerima variran je u opsegu od 40 do 90 mas.%. Struktura, molarne mase i kristaliničnost dobijenih kopolimera su određeni FTIR, ^{1}H- i 2D-NMR spektroskopijom i GPC i DSC analizama, redom. Određivanje slobodne površinske energije je pokazalo prisustvo hidrofobnog (siloksanskog) dela na površini, dajući izrazito hidrofobnu prirodu površini sintetisanih PURs. Merenja količine apsorbovane vode su pokazala da ugradnjom hidrofobnih PPO-PDMS segmenata dolazi do smanjivanja količine apsorbovane vode u kopolimerima. SEM i AFM analize prikazuju da kopolimeri sa nižim sadržajem PPO-PDMS segmenta imaju veći stepen mikrofazne separacije između segmenata. Rezultati dobijeni u ovom radu ukazuju da su sintetisani PURs na bazi PPO-PDMS segmenata, pokazali odgovarajuća površinska i morfološka svojstva, sa značajnim potencijalom za različite primene kao što su hidrofobni premazi u biomedicini.

Ključne reči: Segmentirani poliuretani • Poli(dimetilsiloksani)• 2D-NMR spektroskopija • Površinska energija • Morfologija